ACCOUNTING FOR GROUND MOTION SPECTRAL SHAPE CHARACTERISTICS IN STRUCTURAL COLLAPSE ASSESSMENT THROUGH AN ADJUSTMENT FOR EPSILON

Curt B. Haselton[1], Jack W. Baker[2], Abbie B. Liel[3], and Gregory G. Deierlein[4]

[1] *Department of Civil Engineering, California State University Chico, Chico, CA 95929, USA*
[2] *Department of Civil and Environmental Engineering, Stanford University, Stanford, CA 94305, USA*
[3] *Dept. of Civil, Environmental, and Arch. Engr., University of Colorado, Boulder, CO 80309, USA*
[4] *Department of Civil and Environmental Engineering, Stanford University, Stanford, CA 94305, USA*

ABSTRACT

One of the challenges in assessing structural collapse performance is the appropriate selection of ground motions for use in the nonlinear dynamic collapse simulation. The ground motions should represent characteristics of extreme ground motions that exceed the ground motion intensities considered in the original building design. For modern buildings in the western United States, ground motions that cause collapse are expected to be rare high-intensity motions associated with a large magnitude earthquake.

Recent research has shown that rare high-intensity ground motions have a peaked spectral shape that should be considered in ground motion selection and scaling. One method to account for this spectral shape effect is through selection of a set of ground motions that is specific to the building's fundamental period and the site hazard characteristics. This selection presents a significant challenge when assessing the collapse capacity of a large number of buildings or for developing systematic procedures, since it implies the need to assemble specific ground motion sets for each building. This paper proposes an alternative method, whereby a general set of far-field ground motions is used for collapse simulation, and the resulting collapse capacity is adjusted to account for spectral shape effects that are not reflected in the ground motion selection. The simplified method is compared with the more direct record selection strategy, and results of the two approaches show good agreement.

KEY WORDS: Ground motions, spectral shape, epsilon, collapse assessment, performance assessment, ATC-63, FEMA P695.

INTRODUCTION AND GOALS OF STUDY

One of the challenges in assessing structural collapse capacity by nonlinear dynamic analysis is the selection and scaling of ground motions for use in analysis. Baker and Cornell (2006) have shown that spectral shape, in addition to ground motion intensity, is a key characteristic of ground motions affecting the structural response. In particular, for a given ground motion hazard level (e.g. 2% chance of exceedence in 50 years), the shape of the *uniform hazard spectrum (UHS)* can be quite different from the shape of the *mean (or "expected") response spectrum* of a real ground motion having an equally high spectral amplitude at a single period (Baker 2005, Baker and Cornell 2006). Spectral shape characteristics are especially important for structural collapse assessments because it is at high amplitudes that these differences are most significant.. Therefore, when assessing the probability of collapse under high-amplitude motions, the choice of ground motions significantly impacts the collapse assessment.

To illustrate the distinctive spectral shape of rare ground motions, Figure 1 shows the acceleration spectrum of a Loma Prieta ground motion[1]. This spectrum has a rare spectral intensity at 1.0 second of 0.9g, which has only 2% chance of exceedance in 50 years. The figure also shows the mean expected spectrum predicted by Boore et al. (1997) attenuation prediction, consistent with the event magnitude, distance, and site characteristics associated with this ground motion. Figure 1 shows that this extreme ground motion has a much different shape than the mean predicted spectrum. In particular, the spectrum for this record has a "peak" from approximately 0.6 to 1.8 seconds and lower intensities (relative to the predicted spectrum) at other periods. The intensity at 1.0 second, exceeded with 2% likelihood in 50 years, is in the peaked region of the spectrum and at this period the observed Sa(1s) = 0.9g is much higher than the mean expected Sa(1s) = 0.3g; at other periods away from the peak, spectral values are closer to the mean expected Sa. This peaked shaped arises because ground motions that have an above average intensity do not necessarily have equally large intensities at other periods.

At a 1.0 second period, the spectral value of the Loma Prieta record is 1.9 standard deviations above the predicted mean spectral value from the attenuation relationship, so this

[1] This motion is from the Saratoga station and is owned by the California Department of Mines and Geology and included in the PEER NGA database (PEER 2008). For this illustration, this spectrum was scaled by a factor of +1.4. This scaling is for illustration purposes only, and epsilons should be computed using unscaled spectra.

record is said to have "ε = 1.9 at 1.0 second." ε (epsilon) is defined as the number of logarithmic standard deviations between the observed spectral value and the mean Sa prediction from an ground motion prediction ("attenuation") model. Similarly, this record has ε = 1.1 at 1.8 seconds. Thus, the parameter ε is a function of the ground motion record, the ground motion prediction model to which it is compared, and the period of interest.

Just as ε is a function of period, the relationship between ε and spectral shape depends on the period being considered. For example, a motion with ε(1s) = 2.0 would tend to have a peak near a period of one second, and a motion with ε(2s) = 2.0 would tend to have a peak near a period of two seconds. Since ground motions are inherently random, this relationship between ε and the spectral shape (as shown in Figures 1 and 2) is not necessarily evident for individual ground motions, but is clearly seen (and statistically defensible) when examining average trends in large data sets of recorded ground motions (Baker and Jayaram 2008).

The "peaked" spectral shape of rare ground motions observed in Figure 1 is general to non-near-field sites in coastal California. In particular, such sites typically exhibit values of ε between 1 and 2 for the motions with 2% in 50 year intensity levels. These positive ε arise from the fact that the return period of the ground *motion* (i.e. 2475 years for a 2% in 50 year motion) is much longer than the return period of the *earthquake* that causes the ground *motion* (i.e. typical *earthquake* return periods that govern the high seismic hazard are 150-500 years in California). Accordingly, record selection for structural analyses at such sites should reflect the expectation of ε = 1 to 2 for 2% in 50 year motions.

This paper focuses on consideration of spectral shape through the parameter ε, for purposes of collapse assessment through nonlinear dynamic analysis. Prediction of structural collapse requires a set of ground motions, where the amplitude of each ground motion in the set is scaled to increasing intensity until it causes collapse. The collapse capacity of an individual ground motion record is denoted by the corresponding intensity, based on the spectral acceleration at the first-mode period of the building, $S_{a,col}(T_1)$. The structure's collapse capacity is then defined by the mean[2] and dispersion of the collapse capacities of the individual records. Note that the proposed approach for scaling records and characterizing spectral shape through the ε parameter is based on the defining the ground motion intensities based on $Sa(T_1)$.

As described later, previous research has shown that consideration of this peaked spectral shape significantly increases the computed collapse capacity of a structure relative to results

[2] Strictly speaking, the "mean" used in this paper is the geometric mean (the exponential of the mean of the logarithms). This is equal to the median of a lognormal distribution, so it is also sometimes referred to as the "median". This definition of "mean" is used throughout this paper.

obtained using motions without a peaked spectral shape. For cases where these rare motions (those with ε values approaching 2.0) govern the performance assessment, such as when assessing collapse risk of modern buildings in seismic regions of California, properly accounting for this expected +ε is critical.

The most direct approach to account for spectral shape in structural analysis is to select ground motions that have $\varepsilon(T_1)$ values that match the target $\varepsilon(T_1)$ obtained from hazard analysis for the intensity level of interest, measured at the fundamental period of the structure. An alternative approach is to select and scale ground motions by an intensity measure other than $Sa(T_1)$, which accounts for spectral shape in either an implicit or explicit manner. Possible intensity measures include inelastic spectral displacement (Tothong 2007) or Sa values averaged over a period range (Baker and Cornell 2006). However, since the $Sa(T_1)$ intensity measure is widely used to describe the seismic hazard, the goal of this study is to develop an alternative approach to define and characterize the ground motions for analysis.

The proposed approach is intended to (1) permit the use of a general ground motion set for structural analysis, selected independently of ε values, and (2) then correct the collapse capacity estimates to account for spectral shape. This adjustment is based on $\varepsilon(T_1)$, which is computed for a given site and hazard level through dissagregation of the seismic hazard for the site. Development of this proposed approach was motivated by related studies (FEMA 2008; Haselton and Deierlein 2007, chapters 6-7) that involved assessing the collapse safety of a large set of buildings with differing fundamental periods. Owing to the large number of buildings and a desire to generalize the site characteristics in terms of the Seismic Design Categories, selecting unique ground motion sets for each of the buildings was not feasible.

This paper begins by discussing how spectral shape and ε are related, and then illustrates how spectral shape affects the calculated structural collapse capacity. Next considered are the representative spectral shapes and ε values expected for various sites and hazard levels. A regression method is proposed to account for the effects of spectral shape on collapse by applying a correction factor to the mean collapse capacities obtained using a generic ground motion record set. The regression method is then applied to 111 buildings for the purpose of developing a simplified method to adjust the collapse capacity through an ε correction factor.

PREVIOUS RESEARCH ON THE EPSILON PARAMETER AND SPECTRAL SHAPE EFFECTS ON COLLAPSE ASSESSMENT

How Spectral Shape Relates to the Epsilon Values of Ground Motions

Figure 1 showed the spectral shape of a single Loma Prieta ground motion record that is consistent with a 2% in 50 year intensity level at 1.0 second and has $\varepsilon(1s) = 1.9$. This figure suggests that a positive ε value tends to be related to a peak in the acceleration spectrum around the period of interest. Recent studies have verified the statistical robustness of this relationship between a positive ε and a peaked spectral shape using multiple ground motions. To illustrate, Figure 2 compares the mean spectral shape of three ground motion sets[3]: (1) a set selected without regard to ε (General Far-Field Set, described in FEMA 2008), (2) a set selected to have $\varepsilon(1s) = +2$, and (3) a set selected to have $\varepsilon(2s) = +2$. The General Far-Field Set is approximately epsilon-neutral. To facilitate comparison, these record sets are scaled such that the mean Sa(1s) for set (2) and Sa(2s) for set (3) are matched to the respective values of set (1). Figure 2 shows that the spectral shapes are distinctly different when the records are selected with or without regard to ε. When the records have positive ε values at a specified period, their spectra tend to have a peak at that period. This shape is much different than a standard uniform hazard spectral shape. Baker and Cornell (2006) have developed a statistically rigorous method to predict this expected spectral shape, which is termed the Conditional Mean Spectrum (CMS) because it is conditioned on a Sa value at a specified period.

How Spectral Shape (Epsilon) Affects Collapse Capacity

Selecting ground motions with peaked spectral shapes typical of rare ground motions, as represented by positive $\varepsilon(T_1)$ values, has been shown to significantly increase collapse capacity predictions (where capacity is defined in terms of $Sa(T_1)$). Conceptually, this difference in collapse capacity can be explained by comparing the spectral shapes of the Epsilon Neutral Set (1) and the Positive Epsilon Sets (2) or (3) shown in Figure 2. For example, if a building period is 1.0 second and the ground motion records are scaled to a common value of Sa(1s), the spectral values of the Positive Epsilon Set (2) are smaller than those of the Epsilon Neutral Set (1) for $Sa(T > 1s)$. The spectral values at longer periods are significant since the effective period will elongate as the structure becomes damaged. Similarly, the smaller spectral values for shorter

[3] These ground motion sets contain 78 motions, 20 motions, and 20 motions, respectively.

periods (T < 1s) for the Positive Epsilon Set (2) are significant since they will impact the contribution of higher modes with $T < T_1$.

Four studies have documented the effect of epsilon on nonlinear collapse simulations. Baker and Cornell (2006) studied the effects of various ground motion properties on the collapse capacity of a seven-story non-ductile reinforced concrete (RC) frame building with a fundamental period (T_1) of 0.8 seconds. They found that the mean collapse capacity increased by a factor of 1.7 when an $\varepsilon(0.8s) = 2.0$ ground motion set was used in place of a set selected without regard to epsilon (which has mean $\varepsilon(0.8s) = 0.2$). Goulet et al. (2006) studied the collapse safety of a modern four-story RC frame building with a period of $T_1 = 1.0$ seconds, and compared the collapse capacities for a ground motion set with a mean $\varepsilon(1.0s) = 1.4$ and another set that had a mean $\varepsilon(1.0s) = 0.4$. The set with $\varepsilon(1.0s) = 1.4$ resulted in a mean collapse capacity that was 1.3 to 1.7 times larger than that of the $\varepsilon(1.0s) = 0.4$ set (where the range was associated with variations in building design and modeling attributes). Haselton and Baker (2006) used a ductile, but degrading, single-degree-of-freedom oscillator, with a period of $T_1 = 1.0$ seconds, to demonstrate that a $\varepsilon(1.0s) = 2.0$ ground motion set resulted in a 1.8 times larger mean collapse capacity as compared to using a ground motion set selected without regard to ε (which has mean $\varepsilon(1.0s) = 0.2$). Likewise, Zareian (2006) investigated the effects that ε has on the collapse capacities of generic frame and wall structures. For a selected eight-story frame and eight-story wall building, he showed that a change from $\varepsilon(T_1) = 0.0$ to $\varepsilon(T_1) = 1.5$ results in a factor of 1.5 to 1.6 increase in mean collapse capacity.

The ε parameter has also been considered for prediction of response from near-fault ground motions, but was found to not fully quantify the impact of forward-directivity velocity pulses on structural response (Baker and Cornell 2008). The approach proposed in this paper should not be applied to near-fault motions with large forward-directivity velocity pulses.

WHAT EPSILON VALUES TO EXPECT FOR A SPECIFIC SITE AND HAZARD LEVEL

Illustration of Concept using a Characteristic Event

To illustrate the relationship between expected ε, site, and hazard level, consider an idealized site where the ground motion hazard is dominated by a single characteristic event:

- Characteristic event return period = 200 years
- Characteristic event magnitude = 7.2
- Closest distance to fault = 11.0 km
- Site soil conditions – V_{s_30} = 360 m/s

- Building fundamental period of interest = 1.0 second

Figure 3 shows the predicted mean spectrum and spectra for mean +/- one and two standard deviations (i.e. +/- 1ε and +/- 2ε), given occurrence of the characteristic event. The mean predicted ground motion is Sa(1s) = 0.40g using the Boore et al. (1997) attenuation model. This figure also includes a superimposed lognormal distribution of Sa(1s), representing the predicted distribution of Sa(1s) values (with a logarithmic standard deviation of 0.57) expected from an event with this magnitude, distance, etc. The Sa(1s) values associated with less frequent ground motions (i.e. 2% in 50 years) are associated with the upper tail of the distribution of Sa(1s) for this event.

In general, w*hen the return period of the characteristic earthquake (e.g. 200 years) is much shorter than the return period of the ground motion of interest (e.g. 2475 years), then the ground motion of interest will have a positive ε.* This statement is easily illustrated for the idealized site. When a single characteristic event dominates the ground motion hazard, the mean return period (RP) of the ground motion Sa ≥ x is related to the characteristic event as follows:

$$\frac{1}{RP_{Sa \geq x}} = \left(\frac{1}{RP_{CharactersticEvent}} \right) \left(P[Sa \geq x \mid CharacteristicEvent] \right) \quad (1)$$

The return period for a 2% in 50 year motion, computed using the standard Poissonian occurrence assumption, is P(Sa>x in time t) = 1 – exp(-t / $RP_{Sa>x}$), where t= 50 years and P(Sa>x in time t) = 0.02. This results in a return period, $RP_{Sa>Sa2/50,}$ of 2475 years. The return period of the characteristic event is 200 years. From Equation 1 then, (1/2475years) = (1/200years)*(0.081). This means that only 8% of motions that come from the characteristic earthquake are at least as large as the 2% in 50 year motion. From basic probability, this 8% probability of exceedance corresponds to 1.43 standard deviations above the mean value, or ε(1s) = 1.43. Note that a change in site soil conditions would impact the predicted spectral accelerations at the site due to a change in the attenuation prediction, but it would not change the ε value because the ratio of return periods of the ground motion of interest and the return period of the earthquake would be unchanged. The situation is more complicated for realistic sites with more earthquake sources, but in general the ε value associated with a design Sa level does not change significantly when the site conditions are varied.

The expected ε value depends strongly on the return period of the ground motion of interest. Figure 3 shows that a 10% in 50 year motion (return period of 475years) is associated with Sa(1s) = 0.46g and ε(1s) = 0.3. For a much more frequent 50% in 5 year motion (return period of 7.2 years), Sa(1s) = 0.15g and ε(1s) = -1.7. For cases where rare motions drive the

performance assessment, such as with collapse assessment of modern buildings, it is likely that the ground motion will fall into the "positive ε" category.

Equation 1 also shows that the expected ε value depends on the return period of the characteristic event. In coastal California, earthquake return periods of 200 years are common, but in the Eastern United States, large earthquake return periods are longer. These longer return periods in the Eastern United States will cause the expected ε values for extreme (rare) ground motions to be smaller.

Expected Epsilon Values from the United States Geological Survey

Unlike the idealized site considered above, most locations have several causal earthquake sources that contribute significantly to ground motion hazard, as well as having more complex distributions of magnitude. For the general case, expected ε values must be computed by disaggregating the results of seismic hazard analysis.

The United States Geological Survey (USGS) conducted seismic hazard analyses across the United States and used dissagregation to determine the mean ε ($\overline{\varepsilon}_0$) values for various periods and hazard levels of interest (Harmsen et al., 2002; Harmsen 2001). Figure 4 shows the $\overline{\varepsilon}_0$ for a 2% in 50 year Sa(1s) intensity for the Western United States, for site class B (rock sites). Values of $\overline{\varepsilon}_0(1s)$ = 0.50 to 1.25 are typical in most of the Western United States, except for the high seismic coastal regions of California, where the typical values are $\overline{\varepsilon}_0(1s)$ = 1.0 to 1.75 with peak values as high as 2.0. As shown in Figure 5a, in the Eastern United States, typical values of $\overline{\varepsilon}_0(1s)$ are 0.75 to 1.0, with some values reaching up to 1.25. Expected $\overline{\varepsilon}_0(1s)$ values fall below 0.75 for the New Madrid Fault Zone, portions of the eastern coast, most of Florida, southern Texas, and areas in the north-west portion of the map. The effect of period is illustrated by comparing Figure 5a, $\overline{\varepsilon}_0(1s)$, to Figure 5b, for $\overline{\varepsilon}_0(0.2s)$, which shows that typical $\overline{\varepsilon}_0(0.2s)$ are slightly lower and more variable than $\overline{\varepsilon}_0(1s)$.

To further quantify the expected $\overline{\varepsilon}_0$ values in various regions of the United States, the numeric data used to create the above maps were examined. The data consists of expected $\overline{\varepsilon}_0$ values for periods of 0.2 and 1.0 seconds at the centroid of each zip code in the United States. Table 1 summarizes the subsets of these data for seismic design categories B, C, and D, as defined in the International Building Code (ICC 2006). For each of these seismic design categories (SDCs), the table provides average $\overline{\varepsilon}_0$ values and spectral accelerations for four

ground motion hazard levels: 10%, 2%, 1%, and 0.5% in 50 years. The number of zip codes in each SDC, which is a general measure of building inventories, is also listed.

Since the fault characteristics on the western coast of the United States vary from those in other parts of the country (e.g. the recurrence intervals of seismic events is shorter), Table 1 also shows the data for the SDC D sites in California and selected California cities. On average, the $\overline{\varepsilon}_0$ values are consistently higher in California (as compared to other geographic locations of SDC D), and the $\overline{\varepsilon}_0$ values for many of the highly populated California cities are often even higher than the California average. For example, the $\overline{\varepsilon}_0$(1s) values for the 2% in 50 year hazard in San Francisco is 1.5, as compared to the average value for SDC D of 0.99. Values in Oakland, San Jose and Riverside are even higher, ranging between 1.65 and 1.95.

Figure 4, Figure 5, and Table 1 illustrate the expected $\overline{\varepsilon}_0$ values for site class B (rock sites). These values should be generally applicable to other site conditions, provided that the variability of the ground motions is similar to that of site class B. In cases where the variability in the ground motions differs from that of site class B (e.g. soft soil under very high levels of shaking), additional study is required to determine how the expected $\overline{\varepsilon}_0$ values may vary from those for site class B.

Target Epsilon Values

The expected or target $\overline{\varepsilon}_0$ value for building response assessment depends on the site and hazard level of interest. Thus, the target ε should be determined based on the hazard level that corresponds to the building performance level being considered. For example, when computing the probability of collapse under a ground motion with a 2% frequency of exceedence in 50 years, $P[Col|Sa = Sa_{2/50}]$, the appropriate target hazard level is the 2% in 50 year intensity. When computing the mean annual frequency of collapse (λ_{col}), the appropriate target hazard level is more difficult to determine. Ideally, one would increment the target $\overline{\varepsilon}_0$ value for the various levels of Sa when integrating over the hazard curve. Alternatively, as an approximate approach, one could use the target hazard level that most significantly influences λ_{col}, which will be a function of both the site and the collapse capacity of the structure. Haselton and Deierlein (2007, chapter 5) looked at this question for two example four-story RC frame buildings at a site in Los Angeles and, for those buildings and site, the ground motion intensity level at 60% of the mean collapse capacity was the most dominant contributor to the calculation of λ_{col}. In their example,

this corresponded to motions that have roughly 1.5x the spectral acceleration of a 2% in 50 year ground motion with corresponding characteristic ε values typically being larger than two.

APPROACHES TO ACCOUNT FOR EPSILON IN COLLAPSE ASSESSMENT

Two alternative methods of accounting for ε are illustrated by application to the collapse assessment of an eight-story reinforced concrete (RC) frame model. This design and model was developed by the authors in a related study (Haselton and Deierlein 2007, ID 1011 in chapter 6), and consists of a three-bay special moment resisting perimeter frame (SMF) with 6.1 meter (20 foot) bay widths, a tributary seismic mass floor area of 669 square meters (7,200 square feet), and a fundamental period (T_1) of 1.71 seconds. Haselton and Deierlein (2007) provide more details regarding the nonlinear structural modeling and the methodology used for predicting collapse. The site used for this example is in northern Los Angeles, is typical of the non near-field regions of coastal California (see Goulet et al. 2006), and has NEHRP Category D soil. The primary purpose is to compute the conditional collapse probability for a 2% in 50 year ground motion (which is Sa(1.71s) = 0.57g), and hazard disaggregation provides a target epsilon of ε = 1.7 for this level of ground motion.

Method One: Ground Motion Set Selected with the Target Epsilon

One method to account for ε is to select ground motions with ε values that are consistent with those expected for the site and hazard level of interest. For the assumed site in this example, we selected[4] a Positive ε Ground Motion Set to include 20 ground motions that have a mean $\varepsilon(T_1)$ = 1.7 (where T_1 = 1.71 seconds); each individual record has $\varepsilon(T_1) > 1.25$. In addition, we imposed additional selection criteria such as minimum earthquake magnitude and site class. Haselton and Deierlein (2007, chapter 3) document the motions included in this ground motion set and provide the complete list of selection criteria.

Figure 6 shows the resulting collapse capacity distribution predicted by subjecting the eight-story RC SMF to the 20 ground motions of the Positive ε Set. The collapse capacity for a single ground motion record is defined as the minimum $S_a(T_1)$ value that causes the building to become dynamically unstable, as evidenced by excessive drifts. This figure shows both the individual collapse capacities of the 20 records and a fitted lognormal distribution. The mean collapse capacity is $S_{a,col}(T_1)$ = 1.15g, and the standard deviation of the logarithm of collapse

[4] When selecting records, we used the $\varepsilon(T_1)$ values computed using the Abrahamson and Silva ground motion prediction equation (1997).

capacities (denoted $\sigma_{LN(Sa,col)}$) is 0.28. This dispersion, termed record-to-record variability, is associated with variation in ground motion properties other than $Sa(T_1)$. For the 2% in 50 year $Sa(T_1)$=0.57g, the conditional probability of collapse is quite low, equal to 0.5%.

Method Two: General Ground Motion Set with Adjustments for Epsilon

Motivation and Overview of Method

Method One may not be feasible or practical in all situations, as it requires selecting a specific ground motion set for a specified period (T_1) at a specified site with a target ε. For example, related work in the Applied Technology Council 63 Project (FEMA 2008) involves collapse assessment of approximately 100 buildings, with differing fundamental periods, for generic Seismic Design Categories. In such a study, selecting a specific ground motion set for each building is not practical; nor is it desirable since the goal of that project is to generalize the collapse assessment results across Seismic Design Categories.

Method Two uses a general ground motion set, selected without regard to ε values, and then corrects the calculated structural response distribution to account for the $\overline{\varepsilon}_0$ expected for the specific site and hazard level. The method could be applied to all types of structural responses (interstory drifts, plastic rotations, etc.), but this study focuses on prediction of collapse capacity. The method is outlined as follows:

1) Select a general far-field ground motion set without regard to the ε values of the motions (termed the General Set). This set should have a large number of motions to provide a statistically significant sample and ensure that the regression analysis in step (3) is accurate.
2) Calculate the collapse capacity by nonlinear dynamic analyses, using the Incremental Dynamic Analysis (Vamvatsikos and Cornell 2002) method to scale records and organize the results in a cumulative distribution that is characterized by the mean and record-to-record dispersion of collapse capacity.
3) Perform linear regression analysis between the collapse capacity of each record, $LN[S_{a,col}(T_1)]$, and the $\varepsilon(T_1)$ of the record. This establishes the relationship between the mean $LN[S_{a,col}(T_1)]$ and the $\varepsilon(T_1)$ value.
4) Adjust the collapse capacity distribution, using the regression relationship, to be consistent with the target $\varepsilon(T_1)$ for the site and hazard level of interest.

General Far-Field Ground Motion Set and Comparison to Positive ε Set

The General Ground Motion Set used in this study consists of 78 strong far-field motions that were selected without consideration of their ε values. Haselton and Deierlein (2007, chapter 3) document these motions and provide the complete list of selection criteria. A subset of 44 of these ground motions is also used in Applied Technology Council 63 Project (FEMA 2008) as part of a procedure to validate seismic provisions for structural design. The expanded set of 78 records was used to achieve more accurate regression trends between collapse capacity and the ε values, but fewer may suffice. Figure 7 compares the mean response spectra of the General Record Set to the Positive ε Ground Motion Record Set used in Method One. For comparison, both sets have been scaled so that each ground motion has the same $Sa(T_1)$=0.57g at T = 1.71 seconds. The peaked shape of Positive ε Set, relative to the General Set, is evident.

Application of Method Two to Assess Collapse of Eight-Story RC SMF Building

When subjected to General Set, the eight-story RC SMF building (T_1 = 1.71s) has a mean collapse capacity ($\mu_{Sa,col(T_1)}$) of 0.72g and a dispersion in capacity of $\sigma_{LN(Sa,col)}$ = 0.45. The 2% in 50 year intensity for this site is Sa(1.71s) = 0.57g, so the probability of collapse for this level of motion is 29%. Recall that the probability of collapse under the 2% in 50 year motion when analyzed using the Positive ε Set was only 0.5%. Under Method Two the collapse capacity prediction from the General Set still needs to be adjusted to be consistent with the target $\varepsilon(T_1)$.

Shown in Figure 8 is a plot of the collapse capacity, $LN[S_{a,col}(T_1)]$, versus the corresponding $\varepsilon(T_1)$ values for each record. Also shown is a linear regression (Chatterjee et al. 2000) between $LN[S_{a,col}(T_1)]$ and $\varepsilon(T_1)$, which follows an approach previously proposed by Zareian (2006). The relationship between the mean of $LN[S_{a,col}(T_1)]$ and $\varepsilon(T_1)$ can be described as:

$$\mu'_{LN[Sa,col(T_1)]} = \beta_0 + \beta_1 \bullet \varepsilon(T_1) \qquad (2)$$

where β_0 = -0.356 and β_1 = 0.311 in this example. Note that β_1 represents the slope between ε and collapse capacity, such that larger values of β_1 indicate a greater significance of ε in prediction of collapse capacity.

To adjust the mean collapse capacity for the target $\varepsilon(T_1)$ = 1.7, Equation 2 can be evaluated for the target $\bar{\varepsilon}_0(T_1)$, resulting in the following adjusted mean of $LN[S_{a,col}(T_1)]$:

$$\mu'_{LN[Sa,col(1.71s)]} = \beta_0 + \beta_1 \bullet \left[\bar{\varepsilon}_0\left(T_1\right)\right] = -0.356 + 0.311 \bullet [1.7] = 0.173 \qquad (3)$$

The adjusted mean collapse capacity is now computed by taking the exponential of Equation 3,

$$Mean'_{Sa,col(T_1)} = \exp\left(\mu'_{LN[Sa,col(T_1)]}\right) = \exp(0.173) = 1.19g \quad (4)$$

The ratio of adjusted to original mean collapse capacity, is calculated as,

$$Ratio = \frac{\exp\left(\mu'_{LN[Sa,col(T_1)]}\right)}{\exp\left(\mu_{LN[Sa,col(T_1)]}\right)} = \frac{1.19g}{0.72g} = 1.65 \quad (5)$$

where $\mu_{LN[Sa,col(T_1)]}$ is computed directly from the collapse simulation results using the General Set of ground motions and $\mu'_{LN[Sa,col(T_1)]}$ is the value adjusted by the regression analysis for the target $\bar{\varepsilon}_0(T_1)$ value. The calculated increase in mean collapse capacity from 0.72g to 1.19g (a ratio of 1.65) has a significant impact on collapse performance assessment.

The dispersion in collapse capacity computed directly from the records is $\sigma_{LN(Sa,col(T1))}$ = 0.45, but this is also reduced by the adjustment to the target $\bar{\varepsilon}_0(T_1)$. This reduced conditional standard deviation can be computed as follows (Benjamin and Cornell, 1970; equation 2.4.82):

$$\sigma'_{LN(Sa,col(T_1))} = \sqrt{\left(\sigma_{LN(Sa,col(T_1)),reg}\right)^2 + \left(\beta_1\right)^2\left(\sigma_\varepsilon\right)^2} \quad (6)$$

where the $\sigma_{LN(Sa,col(T1)),reg}$ = 0.36 is computed from the residuals of the regression analysis shown in Figure 8, and σ_ε is the standard deviation of the $\varepsilon(T_1)$ values from dissagregation for a site and hazard level. For the example site used in this study, σ_ε is estimated to be 0.35 for the 2% in 50 year intensity of ground motion. Equation 7 computes the reduced standard deviation, showing that the original record-to-record dispersion in collapse capacity (i.e. $\sigma_{LN(Sa,col(T1)),reg}$) is more dominant than the effects of dispersion in the expected ε value (i.e. $\sqrt{\beta_1^2\sigma_\varepsilon^2}$).

$$\sigma'_{LN(Sa,col(T_1))} = \sqrt{(0.36)^2 + (0.31)^2(0.35)^2} = 0.38 \quad (7)$$

This reduced dispersion is 15% lower than the dispersion in collapse capacity computed directly from the records, which was $\sigma_{LN(Sa,col(T1))}$ = 0.45. Relative to the increase in mean collapse capacity described above, this decrease in dispersion (from 0.45 to 0.38) has only a moderate impact collapse performance assessment, which is most apparent near the tails of the collapse capacity distribution.

Comparison of the Two Methods

Figure 9 overlays the predicted collapse capacity distributions obtained from Methods One and Two for the 8-story RC frame. The plot also includes the collapse predictions of Method Two before the adjustment for ε. Figure 10 is similar to Figure 8, but for comparison, Figure 10

includes the data for Positive ε Set of ground motions. Together, Figure 9, Figure 10, and Table 2 show that the two methods produce nearly the same results, with the predictions of mean collapse capacity differing by only 4%. The dispersion in collapse capacity ($\sigma_{LN(Sa,col)}$) differs from 0.28 for Method One to 0.38 for Method Two. From the authors' past experience, it is not expected that such a large observed difference occurs in general, and the large difference in dispersion could be due to the smaller number of ground motions in the Positive ε Set for Method One. From Figure 9, the probabilities of collapse associated with the 2% in 50 year motion are similar (0.5% and 2.4%), and when the collapse CDF is integrated with the site hazard curve for the example site, the mean annual rates of collapse (λ_{col}) differ only by a factor of 2. These differences are negligible when compared to a factor of 23 in over-prediction of λ_{col} that results from not accounting for the proper ε. In addition, data from Haselton and Deierlein (2007, Chapter 6) show that even minor differences in the structural design can cause the λ_{col} prediction to change by a factor of 1.5 to 2.2, which is similar to the difference in results from the two methods being compared here.

SIMPLIFIED METHOD TO ACCOUNT FOR EFFECTS OF EPSILON

Motivation and Overview

The previous section showed that we can obtain roughly the same collapse capacity predictions by either (a) selecting records with appropriate ε values (Method One) or (b) using general ground motions and then applying a correction factors to account for appropriate ε (Method Two). Method Two is useful because it can account for the target ε without needing to select a unique ground motion set for each building period and site. However, as presented above, Method Two requires significant effort to compute $\varepsilon(T_1)$ values for each ground motion record and then a regression analysis to relate $S_{a,col}(T_1)$ to $\varepsilon(T_1)$. To provide a more practical method for adjusting the collapse capacity, a simplified version of Method Two is proposed for determining the appropriate adjustment factors the collapse capacity distribution without requiring computation of $\varepsilon(T_1)$ values for each record and the regression analysis. Instead, this simplified method uses an empirical equation to estimate β_1 (from Equation 2 above) and an approximate value of $\sigma_{LN(Sa,col(T1))}$ to correct the collapse capacity distribution.

Building Case Studies to Develop the Simplified Method for ε Adjustment

To develop a simplified adjustment approach, the complete Method Two was applied to three sets of RC frame buildings (for a total of 111 buildings), including:

- 65 modern RC SMF buildings ranging in height from 1 to 20 stories. Thirty of these buildings are code-conforming buildings representative of current design (ASCE 7-02 and ACI 318-02) in high seismic regions of California (Haselton and Deierlein 2007, chapter 6). The other thirty-five RC SMF buildings (4- and 12-story) are designed according to revised structural design requirements, including variations to design strength requirements, interstory drifts, and strong column-weak beam ratio (Haselton and Deierlein 2007, chapter 7).
- 20 code-conforming ordinary moment frame (OMF) buildings ranging from 2-12 stories, which are representative of buildings in the eastern United States. These designs were developed as part of the Applied Technology Council 63 Project (FEMA 2008).
- 26 non-ductile RC frame buildings, which are representative of existing 1967-era buildings, ranging from 2-12 stories, in high seismic regions of California (Liel, 2008).

Collapse analysis was conducted for each building and regression analysis applied to $LN[S_{a,col}(T_1)]$ versus $\varepsilon(T_1)$ to determine the factor β_1 (as defined in Equation 2). A selected subset of these values is presented in Table 3. The mean β_1 value for the 65 RC SMF buildings is β_1=0.28. This value is exceptionally stable, with a coefficient of variation value of only 0.14 over the wide variety of buildings of varying heights and design. This stability of the β_1 values indicates that the influence of ε (spectral shape) on collapse capacity is fairly consistent between buildings with similar levels of inelastic deformation capacity. The mean value for the 20 RC OMF buildings is β_1=0.19, which is 40% lower than the more ductile SMF buildings, and the mean value for the 1967-era buildings was β_1=0.18, which is quite similar the RC OMF frames. These lower β_1 values indicate that ε has less influence on the collapse capacities of these RC OMF and 1967-era RC frame buildings, which have less inelastic deformation capacity as compared with the RC SMF buildings. Building deformation capacities, as quantified by the ultimate roof drift ratio, are also reported in Table 3. Note that RDR_{ult} is the roof drift ratio at 20% strength loss, as predicted using static pushover analysis (e.g. RDR_{ult} = 0.047 for the pushover shown in Figure 13). Table 3 shows generally that buildings with larger deformation capacity (RDR_{ult}) have higher values of β_1.

Developing Components of the Simplified Method

Prediction of β_1

The significance of ε, as reflected in the β_1 parameter, is larger for buildings with higher deformation capacity because ductile buildings soften (and thus their effective period increases)

prior to collapse, which makes the spectral shape (specifically spectral values at $T>T_1$) more important to the structural response. The trend between β_1 and RDR_{ult} is illustrated in Figure 11a for four sets of RC SMF buildings, each set with the same height. These data show a trend for deformation capacities up to $RDR_{ult} = 0.04$, and suggest that deformation capacity in excess of this (i.e. $RDR_{ult} > 0.04$) does not influence β_1.

β_1 also tends to be larger for taller buildings, because of the significance of higher mode effects on the dynamic response of tall buildings, thereby making the spectral shape for periods less than T_1 an important consideration. To investigate the impact of building height, separate from deformation capacity, Figure 11b compares the β_1 values for six pairs of 4- and 12-story RC SMF buildings that have the same RDR_{ult} values. These data show a clear trend between β_1 and building height, for 5 of the 6 sets of buildings considered.

To create the predictive equation for β_1, standard linear regression analysis was used to relate calculate $LN(\beta_1)$ as a function of RDR_{ult} and building height, based on the data from all 111 buildings (Chatterjee et al 2000). We then applied judgmental corrections to better replicate the trends with deformation capacity and building height (see Figure 11). These corrections were required because of the limited number of data points available to reflect the separate trends of height and building deformation capacity. The functional form of Equation 8 captures the nearly linear effects of height and the nonlinear effects of RDR^*_{ult} for buildings with lower deformation capacity. The resulting equation for β_1 is as follows,

$$\hat{\beta}_1 = (0.4)(N+5)^{0.35}\left(RDR^*_{ult}\right)^{0.38} \qquad (8)$$

where N is the number of stories (limited to $N \leq 20$ based on available data); and RDR_{ult} is the roof drift ratio at 20% base shear strength loss from static pushover analysis ($RDR^*_{ult} = \min(RDR_{ult}, 0.04)$, based on the observation from Figure 11a that the trend saturates at a value of 0.04). It is noted that application of static pushover analysis to taller buildings is limited because of the important impact of higher modes, but it is utilized here to *approximate* the building deformation capacity.

The effects of height and deformation capacity tend to counteract one another, which is why β_1 is fairly consistent for the set of 30 code-conforming RC frame buildings varying from 1-story to 20-stories. In Figure 12, the ratio of observed β_1 to predicted β_1 from Equation 8 is plotted against the building deformation capacity and the number of stories, showing that Equation 8 provides reasonable predictions for most of the 111 buildings used in this study. However, β_1 is significantly under-predicted (i.e. conservative) for three of the 1-story buildings, but is accurate for the fourth 1-story building. It would be useful to extend this study to include a larger number of short period buildings to further validate the proposed relationship.

Prediction of $\sigma'_{LN(Sa,col(T1))}$

The data in Table 3 show that accounting for ε reduces the dispersion in collapse capacity. This reduction in dispersion is reduced by about 10-15% for ductile RC SMF buildings and 5% for non-ductile buildings. For simplicity, it is proposed to ignore this effect and to compute the dispersion directly from the set of General Set of records, i.e., to assume that

$$\sigma'_{LN(Sa,col(T_1))} \approx \sigma_{LN(Sa,col(T_1))} \tag{9}$$

Proposed Simplified Method

The section summarizes the proposed Simplified Method for adjusting collapse capacity to reflect appropriate spectral shape with illustration for a 4-story RC SMF space frame.

Step 1. Build a structural model that is robust and able to simulate structural collapse. Calculate the building period and perform a static pushover analysis (with a reasonable load pattern) to determine the roof drift ratio at 20% lateral strength loss (RDR_{ult}). For this example 4-story RC SMF building, $T_1 = 0.94$ seconds. The static pushover analysis was based on the lateral load pattern recommended by ASCE 7-05 (ASCE 2005), resulting in the pushover curve shown in Figure 13 where $RDR_{ult} = 0.047$.

Step 2. Perform nonlinear dynamic analyses to predict collapse capacity using the FEMA P695 (FEMA 2008) far-field set of 44 records[5]. Compute the natural logarithm of the collapse capacity for each record, and then compute the mean and standard deviation of these values for all records (i.e. $\mu_{LN[Sa,col(T1)]}$ and $\sigma_{LN[Sa,col(T1)]}$). For the example 4-story RC SMF building, the results of the nonlinear dynamic collapse analyses are shown as follows.

$$\mu_{LN[Sa,col(T1)]} = \mu_{LN[Sa,col(0.94s)]} = 0.601 \tag{10}$$

$$\sigma_{LN[Sa,col(T1)]} = \sigma_{LN[Sa,col(0.94s)]} = 0.40 \tag{11}$$

The mean collapse capacity can be computed from the logarithmic mean as follows:

$$Mean_{[Sa,col(0.94s)]} = \exp\left(\mu_{LN[Sa,col(0.94s)]}\right) = 1.82g \tag{12}$$

Step 3. Estimate β_1 using Equation 8. For the 4-story RC SMF example:

$$\hat{\beta}_1 = (0.4)(N+5)^{0.35}\left(RDR^*_{ult}\right)^{0.38} \tag{13}$$

[5] Alternatively, one could use the larger General Set of 78 records. However, our analyses have shown that the two sets result in about the same mean and dispersion of collapse capacity. The reason for using the larger set in this paper was to better predict the regression line between $LN(S_{a,col}(T_1))$ and $\varepsilon(T_1)$; this additional information is not required in the simplified method.

$$RDR^{*}_{ult} = 0.04 \tag{14}$$

$$\hat{\beta}_1 = (0.4)(4+5)^{0.35}(0.04)^{0.38} = 0.254 \tag{15}$$

Step 4. Determine the target mean ε value ($\varepsilon(T_1)_{,target}$) for the site and hazard level of interest. For illustration the 4-story RC SMF, we assume that the target is ($\varepsilon(T_1)_{,target}$) = 1.9, which is similar to an expected ε value of a 2% in 50 year ground motion level in Riverside California (see Table 1).

Step 5. Adjust for the difference between the target ε value and the ε values of the ground motions used in the collapse simulation. To do this, the mean ε value from the General Set of records ($\bar{\varepsilon}(T_1)_{,records}$) is required. Shown in Figure 14 is a plot of mean ε values for the General Set of records. From this figure one can read the value of $\bar{\varepsilon}(T_1)_{,records}$. For the example building, T_1 = 0.94 seconds and the collapse simulation is based on the 78 General Record set, so $\bar{\varepsilon}(T_1)_{,records}$ = 0.17. In general, any set of ground motions could be used, provided that $\bar{\varepsilon}(T_1)_{,records}$ is known.

Step 6. Compute the adjusted mean collapse capacity. This adjusted capacity accounts for the difference between the mean ε of the General Set of records ($\bar{\varepsilon}(T_1)_{,records}$) and the target ε values that comes from dissagregation ($\bar{\varepsilon}_0(T_1)$). The following equations illustrate this calculation for the example 4-story RC SMF:

$$\mu'_{LN[Sa,col(T1)]} = \mu_{LN[Sa,col(T1)]} + \hat{\beta}_1\left(\bar{\varepsilon}_0(T_1) - \bar{\varepsilon}(T_1)_{,records}\right) \tag{16}$$

$$\mu'_{LN[Sa,col(0.94s)]} = 0.601 + 0.254(1.9 - 0.17) = 1.040 \tag{17}$$

$$Mean'_{Sa,col(0.94s)} = \exp\left(\mu'_{LN[Sa,col(0.94s)]}\right) = \exp(1.040) = 2.83g \tag{18}$$

As additional information, the ratio of the adjusted to unadjusted mean collapse capacity can also be computed using Equations 12 and 18, as follows:

$$Ratio = \frac{Mean'_{Sa,col(T_1)}}{Mean_{[Sa,col(T_1)]}} = \frac{Mean'_{Sa,col(0.94s)}}{Mean_{[Sa,col(0.94s)]}} = \frac{2.83g}{1.82g} = 1.55 \tag{19}$$

Step 7. Compute the dispersion in collapse capacity using Equation 10. In this step, we propose to simply use the value computed directly from the nonlinear dynamic analyses, where,

$$\sigma'_{LN(Sa,col(T_1))} \approx \sigma_{LN(Sa,col(T_1)} = 0.40 \tag{20}$$

Comparison Between Simplified and Full Method Two

For comparison, applying Method Two to this same building (based on data for this building from Haselton and Deierlein 2007, chapter 3) would result in very similar results to the Simplified Method. The full regression analysis results yield $\beta_1 = 0.257$, which agrees very well with the simplified value of $\hat{\beta}_1 = 0.254$. The corresponding mean collapse capacity from the full Method Two is 2.63g as compared to the simplified value of 2.83g. This difference of about 8% is reasonable for most applications, particularly in contrast to the alternative of neglecting the spectral shape effects. The calculated dispersion from the full Method Two is $\sigma'_{LN(Sa,col(T_1))} = 0.35$, which is about 10% lower than the slightly conservative value of 0.40 used in the simplified method. The conditional probability of collapse for the 2% in 50 year ground motion level (Sa(0.94s) = 0.87g) is effectively zero in both cases (0.2% and 0.1%).

SUMMARY, LIMITATIONS, AND FUTURE WORK

Consideration of spectral shape is critical in selection and scaling of ground motions for use in collapse assessment by nonlinear dynamic analysis. As proposed herein, the spectral shape characteristics can be included in collapse assessment through consideration of the parameter ε, which is a measure of how ground motion acceleration spectra vary from the mean predictions provided by ground motion attenuation relationships. For an example 8-story RC SMF building, accounting for the ε adjustment increased the mean collapse capacity by a factor of 1.6, decreased the conditional probability of collapse for the 2% in 50 year ground motion, $P[C|Sa_{2/50}]$, from 29% to 0.5%, and decreased the mean annual frequency of collapse by a factor of 23.

The most direct approach to account for the ε-effect in collapse assessment is to select ground motions whose $\varepsilon(T_1)$ values match those of the building site, collapse Sa intensity, and structural period of interest. However, this approach is often impractical and sometimes infeasible when assessing the collapse performance of buildings with varying vibration periods at multiple sites and under varying ground motion intensities. An alternative simplified approach is proposed that applies an adjustment to the collapse capacity, based on the target $\varepsilon(T_1)$, which eliminates the necessity of considering $\varepsilon(T_1)$ in selection of the ground motion records. Two variants of the ε-adjustment method are proposed, one of which is a simplified version of the other.

To develop and validate the proposed ε-adjustment method, the collapse capacities of three sets of RC frame buildings were investigated including (a) 65 modern RC ductile special moment frames, (b) 26 non-ductile 1967-era RC frames, and (c) 20 RC limited-ductility ordinary

moment frames. These 111 buildings range in height from 1 to 20 stories with fundamental vibration periods ranging from 0.4 to 4.4 seconds (with most periods being less than 3.0 seconds). We simulated the collapse capacity of each building for 78 ground motion records, and then used regression analysis to find the relationship between the collapse intensity, $S_{a,col}(T_1)$, and the corresponding $\varepsilon(T_1)$ for each building and ground motion. The resulting collapse capacities calculated through this regression technique (called Method Two in this paper) are shown to agree well with the results obtained by using a ground motion set selected to have the target ε.

A simplified version of Method Two is developed, in which a semi-empirical equation (Equation 8) is used to calculate the $\varepsilon(T_1)$ collapse adjustment factor in lieu of conducting regression analyses. This equation is developed based on generalized regression analyses conducted using data from the collapse capacities of the 111 case study buildings. The resulting semi-empirical equation (Equation 8) reflects variations in building height and deformation capacity, the latter of which is determined using a pushover analysis. The proposed Simplified Method allows the analyst to use a general ground motion set, selected without regard to ε, to calculate an unadjusted building collapse capacity by using nonlinear dynamic analysis, and then to correct this capacity using an adjustment factor to reflect the expected $\varepsilon(T_1)$ for the building site and collapse hazard intensity, $S_{a,col}(T_1)$. The general set of far-field strong ground motions from the FEMA P695 (FEMA 2008) are suggested for applying this simplified procedure.

Whereas the full Method Two is general in its applicability, the simplified version of the method should only be utilized for structures and ground motions similar to those to which it was developed and calibrated. In terms of structural type, the development was limited to moment frame buildings, ranging in height from 1-20 stories and ranging in periods from 0.4 to 3.0 seconds. The ground motions and target ε values used in the study are generally representative of Site Classes B, C, and D, with a focus on ε values in the range of $\varepsilon = 0$ to +2.0. The simplified Method Two should not be used for other site classes (particularly soft soil sites) or for sites with target ε values outside of the noted range without appropriate ground motion selection and recalibration of the adjustment factor for these conditions.

An implicit assumption of the proposed techniques is that the spectral acceleration at the fundamental period of the building, $Sa(T_1)$, is used to scale the ground motions and quantify the collapse intensity. This assumption is fundamental to the definition of the ε adjustment factor. For tall or irregular buildings, there may be multiple dominant periods of response, the effects of which warrant further study. For example, if three periods dominate the structural response of a tall building, perhaps the collapse assessment could be completed once for each of the three periods, and the controlling case could be used.

This work is currently being adapted for use in the ATC Project 63 (FEMA 2008), which is aimed at providing codified guidelines and procedures for the collapse capacity prediction of buildings. The goal of the ATC project is to use the codified collapse prediction procedures to determine the appropriate prescriptive design requirements (e.g. the R factor) for newly proposed structural systems.

This research could also be extended to look more closely at impacts of spectral shape (ε) on the collapse behavior of short period buildings. Additionally, this method was developed with the primary goal of generalized collapse assessment to evaluate the relative safety among groups of buildings located on comparable sites. Further work would be useful to extend this method for case-specific collapse analysis of specific buildings at particular sites. This extension may involve selection of records to match the target spectral shape directly (Baker and Cornell 2006), including factors such as site class, which may significantly alter the shape.

ACKNOWLEDGEMENTS

This research was supported primarily by the Earthquake Engineering Research Centers Program of the National Science Foundation, under award number EEC-9701568 through the Pacific Earthquake Engineering Research Center (PEER). The research findings were also supported by related studies conducted for the ATC 63 Project, supported by the Federal Emergency Management Agency. Any opinions, findings, and conclusions or recommendations expressed in this material are those of the authors and do not necessarily reflect those of the National Science Foundation or the Federal Emergency Management Agency.

The authors would also acknowledge the contributions of (1) Nico Luco, Stephen Harmsen, and Arthur Frankel of the United States Geological Survey (USGS) who provided mean $\overline{\varepsilon}_0$ data used in this research, (2) the suggestions and advice of Dr. Charlie Kircher and other members of the ATC 63 project, and (3) the assistance of Jason Chou and Brian Dean in conducting the structural collapse analyses used in this study.

REFERENCES

Abrahamson N.A. and W.J. Silva (1997). Empirical response spectral attenuation relations for shallow crustal earthquake, Seismological Research Letters, 68 (1), 94-126.

Baker, J.W. and N. Jayaram (2008). Correlation of spectral acceleration values from NGA ground motion models, *Earthquake Spectra*, 24 (1), 299-317.

Baker, J.W. and C.A. Cornell (2008). Vector-valued intensity measures for pulse-like near-fault ground motions, *Engineering Structures*, 30 (4), 1048-1057.

Baker, J.W. and C.A. Cornell (2006). "Spectral shape, epsilon and record selection", *Earthquake Engr. & Structural Dynamics*, 34 (10), 1193-1217.

Baker, J.W. (2005). *Vector-Valued Ground Motion Intensity Measures for Probabilistic Seismic Demand Analysis*, Ph.D. Dissertation, Department of Civil and Environmental Engineering, Stanford University.

Bazzurro, P. and C.A. Cornell (1999) "Disaggregation of Seismic Hazard," *Bull. Seism. Soc. Am.,* Vol. 89, no. 2, 501-520.

Benjamin, J.R. and C.A. Cornell (1970). Probability, statistics, and decision for civil engineers, McGraw-Hill, New York, 684 pp.

Boore, D.M., W.B. Joyner and T.E. Fumal (1997). Equations for estimating horizontal response spectra and peak accelerations from western North America earthquakes: A summary of recent work, Seismological Research Letters, 68 (1), 128-153.

Chatterjee, S., A.S. Hadi and B. Price (2000). *Regression Analysis by Example*, Third Edition, John Wiley and Sons Inc., New York, ISBN: 0-471-31946-5.

Goulet, C., C.B. Haselton, J. Mitrani-Reiser, J. Beck, G.G. Deierlein, K.A. Porter, and J. Stewart (2007). "Evaluation of the Seismic Performance of a Code-Conforming Reinforced-Concrete Frame Building - from seismic hazard to collapse Safety and Economic Losses", *Earthquake Engineering and Structural Dynamics.*

Federal Emergency Management Agency (FEMA) (2008). ATC-63 Project 90% Draft Report - FEMA P695 *Recommended Methodology for Quantification of Building System Performance and Response Parameters*, Prepared by the Applied Technology Council, Redwood City, CA.

Harmsen, S.C., A.D. Frankel and M.D. Petersen (2002). "Deaggregation of U.S. Seismic Hazard: The 2002 Update", U.S. Geological Survey Open-File Report 03-440, http://pubs.usgs.gov/of/2003/ofr-03-440/ofr-03-440.html (last accessed September 12, 2006).

Harmsen, S.C. (2001). "Mean and Modal ε in the Deaggregation of Probabilistic Ground Motion", *Bulletin of the Seismological Society of America*, 91, 6, pp. 1537-1552, December 2001.

Haselton, C.B. and G.G. Deierlein (2007). *Assessing Seismic Collapse Safety of Modern Reinforced Concrete Frame,* PEER Report 2007/08, Pacific Engineering Research Center, University of California, Berkeley, California.

Haselton, C.B., J. Mitrani-Reiser, C. Goulet, G.G. Deierlein, J. Beck, K.A. Porter, J. Stewart, and E. Taciroglu (2008). *An Assessment to Benchmark the Seismic Performance of a Code-Conforming Reinforced-Concrete Moment-Frame Building*, PEER Report 2007/12, Pacific Engineering Research Center, University of California, Berkeley, California.

Haselton, C.B. and J.W. Baker (2006), "Ground motion intensity measures for collapse capacity prediction: Choice of optimal spectral period and effect of spectral shape", *8th National Conference on Earthquake Engineering*, San Francisco, California, April 18-22, 2006.

International Code Council. (2003). *2003 International Building Code,* Falls Church, VA.

Liel, A. B. (2008). Assessing the Collapse Risk of California's Existing Reinforced Concrete Frame Structures: Metrics for Seismic Safety Decisions, Ph.D. Dissertation, Stanford University.

McGuire, R.K. (1995). "Probabilistic seismic hazard analysis and design earthquakes: closing the loop", *Bulletin of the Seismological Society of America*, 85, pp. 1275-1284.

PEER (2008). *Pacific Earthquake Engineering Research Center: PEER NGA Database*, University of California, Berkeley, http://peer.berkeley.edu/nga/ (last accessed July 2008).

Tothong, P. (2007). *Probabilistic Seismic Demand Analysis using Advanced Ground Motion Intensity Measures, Attenuation Relationships, and Near-Fault Effects*, PhD Dissertation, Department of Civil and Environmental Engineering, Stanford University.

Vamvatsikos, D. and C.A. Cornell (2002). "Incremental Dynamic Analysis," *Earthquake Engineering and Structural Dynamics*, Vol. 31, Issue 3, pp. 491-514.

Zareian, F. (2006). *Simplified Performance-Based Earthquake Engineering*, PhD Dissertation, Department of Civil and Environmental Engineering, Stanford University.

TABLES

Table 1. Mean predicted $\bar{\varepsilon}_0$ values for periods of 0.2 and 1.0 seconds, sorted by seismic design category, with additional detail given for California sites and selected California cities.

Seismic Design Category	Average ε Values								Average Sa Values								Number of Zip Code Data Points
	ε_0(0.2s)				ε_0(1.0s)				Sa(0.2s) [g]				Sa(1.0s) [g]				
	$\varepsilon_{10/50}$	$\varepsilon_{2/50}$	$\varepsilon_{1/50}$	$\varepsilon_{0.5/50}$	$\varepsilon_{10/50}$	$\varepsilon_{2/50}$	$\varepsilon_{1/50}$	$\varepsilon_{0.5/50}$	$Sa_{10/50}$	$Sa_{2/50}$	$Sa_{1/50}$	$Sa_{0.5/50}$	$Sa_{10/50}$	$Sa_{2/50}$	$Sa_{1/50}$	$Sa_{0.5/50}$	
SDC B	0.14	0.42	0.49	0.55	0.31	0.80	0.94	1.04	0.06	0.18	0.26	0.39	0.02	0.06	0.08	0.11	20,142
SDC C	0.11	0.51	0.63	0.75	0.23	0.74	0.88	1.00	0.11	0.31	0.46	0.66	0.04	0.10	0.14	0.19	7,456
SDC D	0.25	0.88	1.09	1.27	0.33	0.99	1.21	1.39	0.50	1.05	1.35	1.68	0.18	0.38	0.49	0.62	6,461
SDC D, CA	0.67	1.12	1.30	1.46	0.89	1.35	1.52	1.67	0.81	1.42	1.73	2.07	0.31	0.55	0.68	0.81	2,273
San Francisco, SDC D	0.88	1.57	1.79	1.95	0.75	1.50	1.75	1.94	1.13	1.78	2.07	2.37	0.52	0.89	1.07	1.25	16
Oakland, SDC D	0.75	1.50	1.75	2.00	0.95	1.65	1.89	2.13	1.56	2.60	3.07	3.55	0.60	1.01	1.21	1.41	10
Berkeley, SDC D	0.67	1.41	1.66	1.91	0.90	1.58	1.82	2.04	1.55	2.62	3.11	3.65	0.59	1.01	1.22	1.43	3
San Jose, SDC D	1.11	1.67	1.84	1.94	0.97	1.64	1.86	2.06	1.23	1.92	2.24	2.59	0.47	0.79	0.94	1.10	29
Los Angeles, SDC D	0.66	1.17	1.39	1.62	0.90	1.33	1.50	1.70	1.12	1.99	2.43	2.92	0.39	0.69	0.85	1.02	58
Riverside, SDC D	1.35	1.77	1.87	1.88	1.41	1.95	2.12	2.22	1.17	1.74	2.02	2.32	0.47	0.72	0.83	0.94	8

Table 2. Comparison of collapse risks for the example Eight-Story RC SMF Building, predicted using the two proposed methods, as well as without any treatment of ε.

Method	Mean Sa,col(1.71s)	σ_{LN}(Sa,col)	P[C|$Sa_{2/50}$]	λ_{col} [10^{-4}]
Method One	1.15	0.28	0.005	0.28
Method Two	1.20	0.38	0.024	0.50
Predictions with no ε Adjustment	0.72	0.45	0.29	6.3
Ratio: Method Two to Method One	1.0	1.2	5	2
Ratio: No Adjustment to Method One	0.63	1.6	58	23

Table 3. Results for a subset of the 111 buildings showing the relationship between building deformation capacity (RDR_{ult}) and β_1, a measure of the significance of $\varepsilon(T_1)$ in collapse capacity predictions. β_1 is obtained from regression analysis.

		RC SMF Buildings			1967-era RC Frame Bldgs.			RC OMF Buildings		
No. of stories	Framing System	RDR_{ult}	β_1	$\sigma_{LN,reg} / \sigma_{LN}$	RDR_{ult}	β_1	$\sigma_{LN,reg} / \sigma_{LN}$	RDR_{ult}	β_1	$\sigma_{LN,reg} / \sigma_{LN}$
2	Perimeter	0.067	0.26	0.82	0.035	0.22	0.86	0.024	0.28	0.95
	Space	0.085	0.26	0.81	0.019	0.16	0.91	0.019	0.09	0.97
4	Perimeter	0.038	0.27	0.83	0.013	0.18	0.90	0.016	0.24	0.92
	Space	0.047	0.26	0.83	0.016	0.20	0.88	0.011	0.27	0.97
8	Perimeter	0.023	0.31	0.81	0.007	0.16	0.97	0.009	0.12	0.82
	Space	0.028	0.32	0.79	0.011	0.18	0.95	0.014	0.19	0.95
12	Perimeter	0.026	0.29	0.84	0.005	0.10	0.97	0.009	0.17	0.97
	Space	0.022	0.25	0.86	0.010	0.16	0.95	--	0.16	--
Mean of this Subset:		0.033	0.27	0.82	0.012	0.17	0.93	0.014	0.18	0.95
Mean of Full Set:		--	0.28	--	--	0.18	--	--	0.19	--

FIGURES

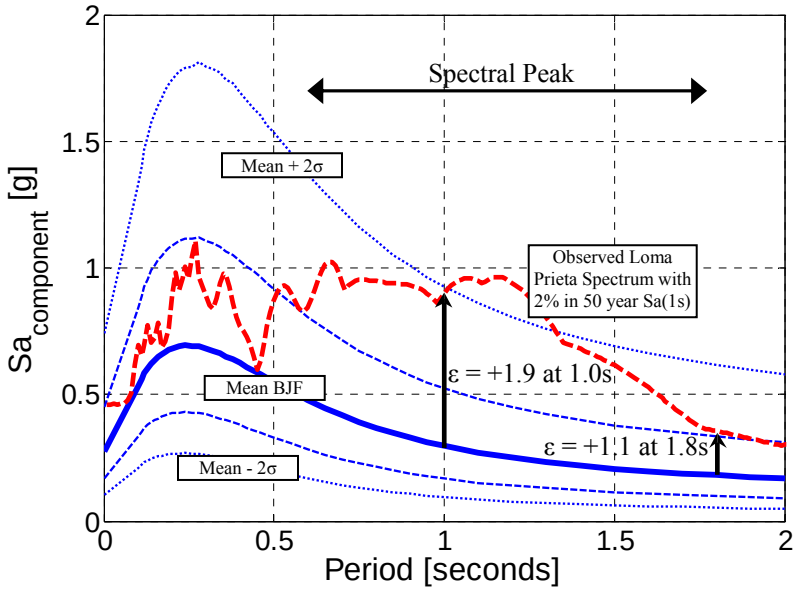

Figure 1. Comparison of an observed spectrum from a Loma Prieta motion with spectra predicted by Boore, Joyner, and Fumal (1997); after Haselton and Baker (2006).

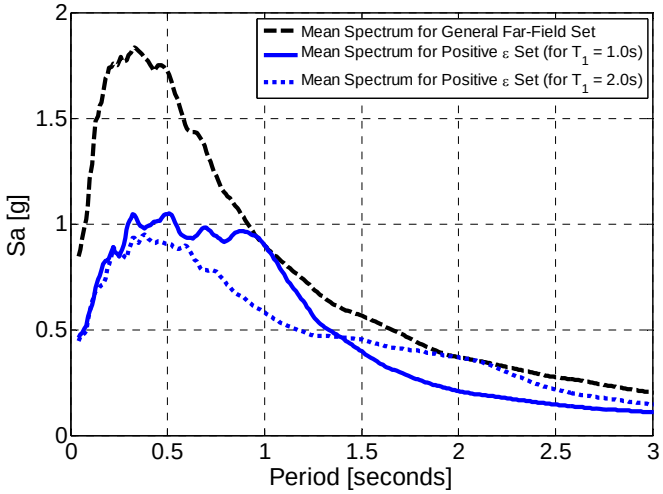

Figure 2. Comparison of spectral shapes of ground motion sets selected with and without considering ε. After Haselton and Baker, 2006.

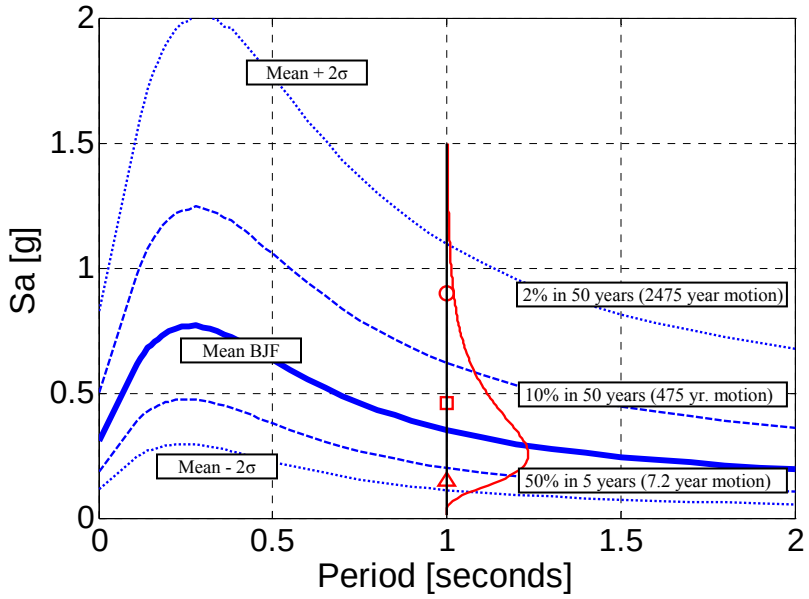

Figure 3. Boore et al. (1997) ground motion predictions for the characteristic event, predicted lognormal distribution at T = 1.0 second, and spectral accelerations for the 2% in 50 year and other hazard levels.

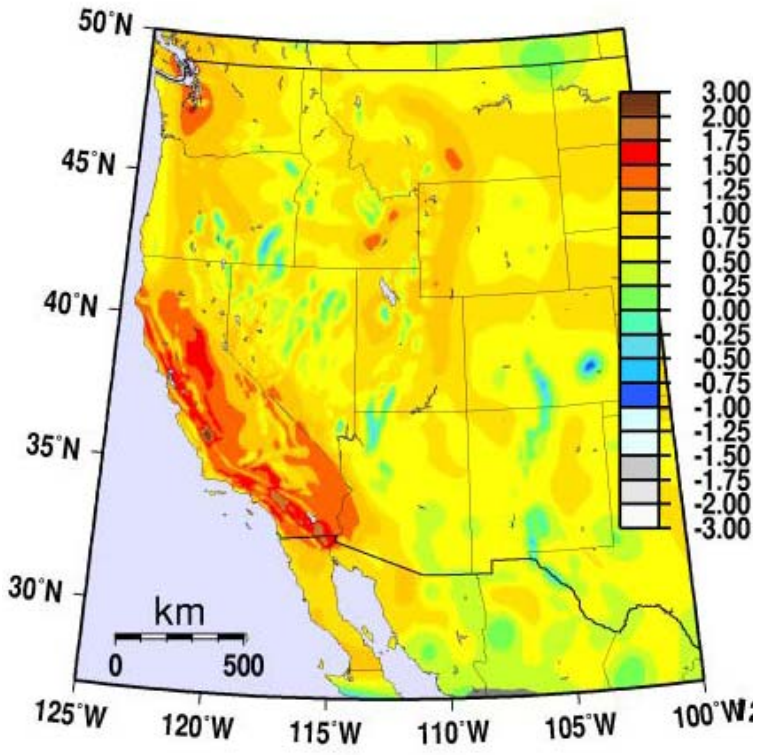

Figure 4. Predicted $\overline{\varepsilon}_0$ values from dissagregation of ground motion hazard, for the Western United States. The values are for a 1.0 second period and the 2% in 50 year motion. After Harmsen et al. 2002.

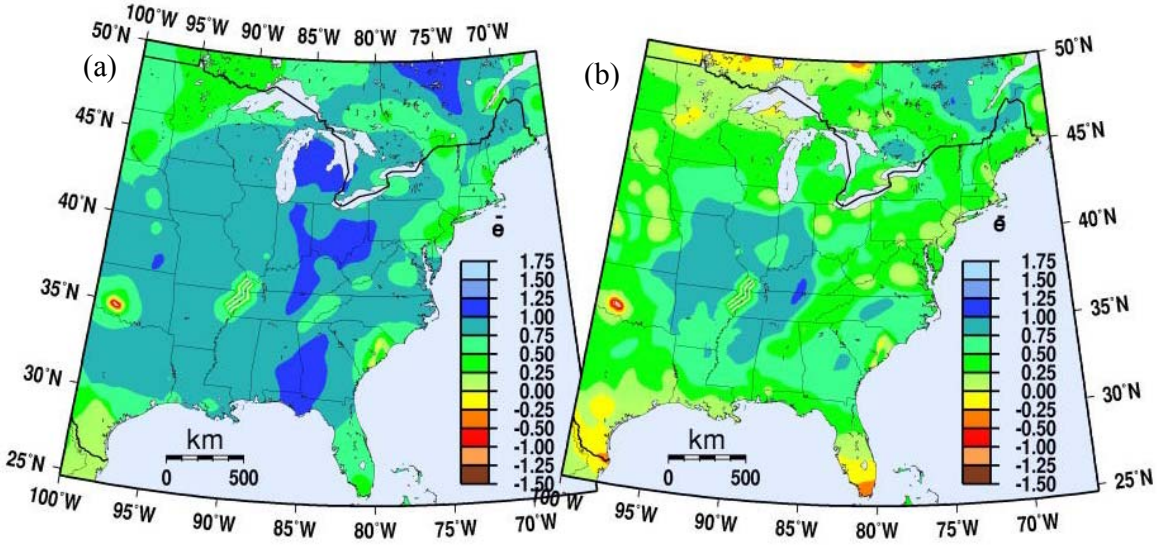

Figure 5. Mean predicted $\overline{\varepsilon}_0$ values from dissagregation of ground motion hazard, for the Eastern United States. The values are for (a) 1.0 second and (b) 0.2 second periods and the 2% in 50 year motion. After Harmsen et al. 2002.

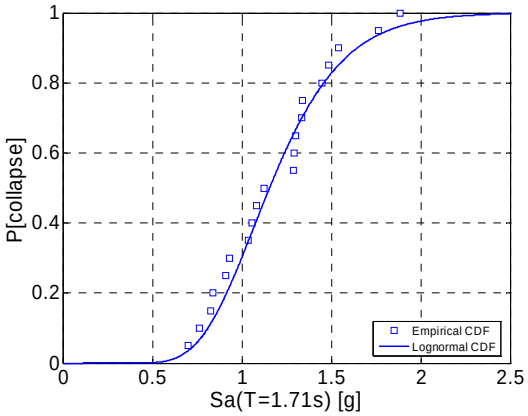

Figure 6. Predicted collapse capacity distribution for the example eight story reinforced concrete frame, computed using the Positive ε Ground Motion Set.

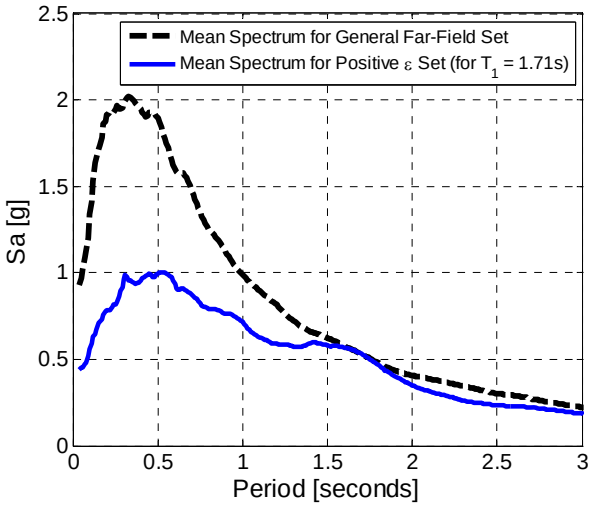

Figure 7. Comparison of mean spectra for the General Set and Positive ε Set of ground motion.

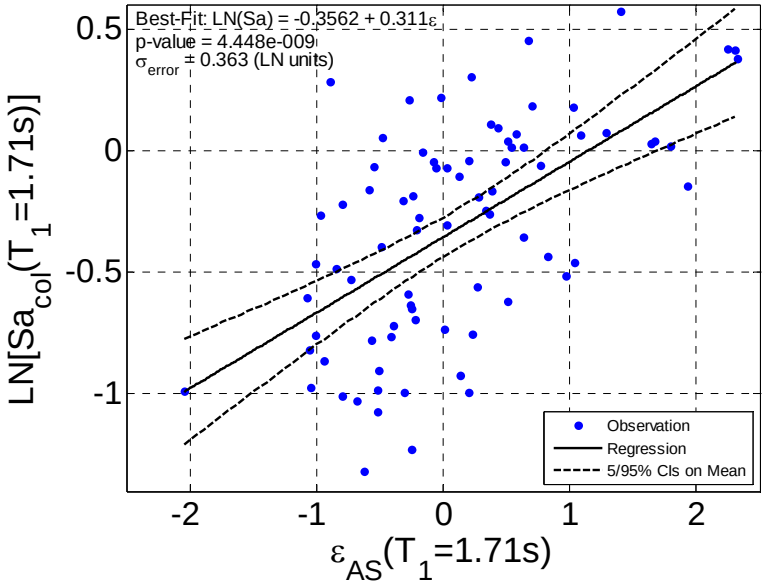

Figure 8. Relationship between collapse capacity (in terms of spectral acceleration) and ε for each ground motion record (computed using Abrahamson and Silva (1997)), including linear regression relating $LN[S_{a,col}(T_1)]$ to $\varepsilon(T_1)$.

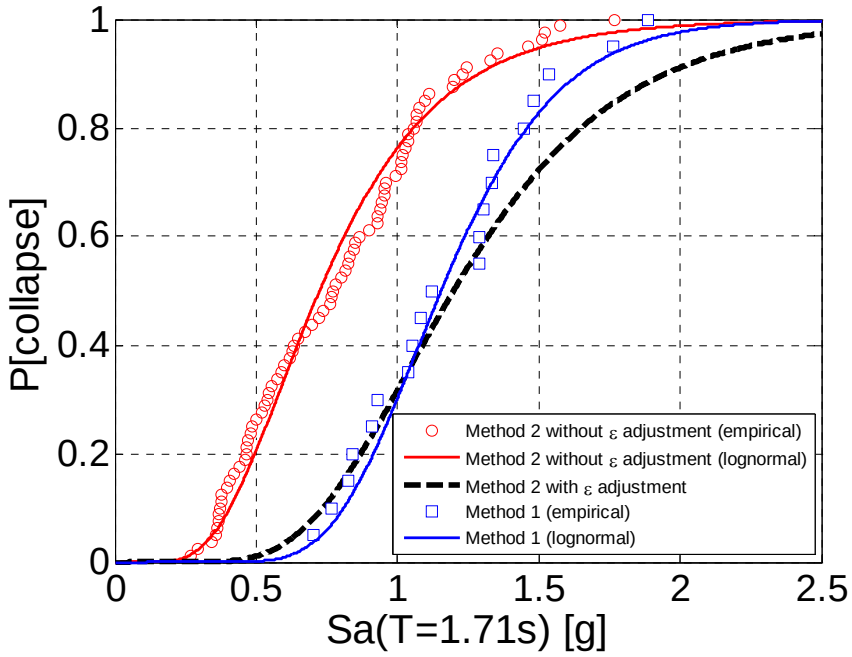

Figure 9. Comparison of collapse capacity distributions predicted using the two methods, where for Method T2 results are shown before and after the adjustment to the target $\bar{\varepsilon}_0(T_1)$.

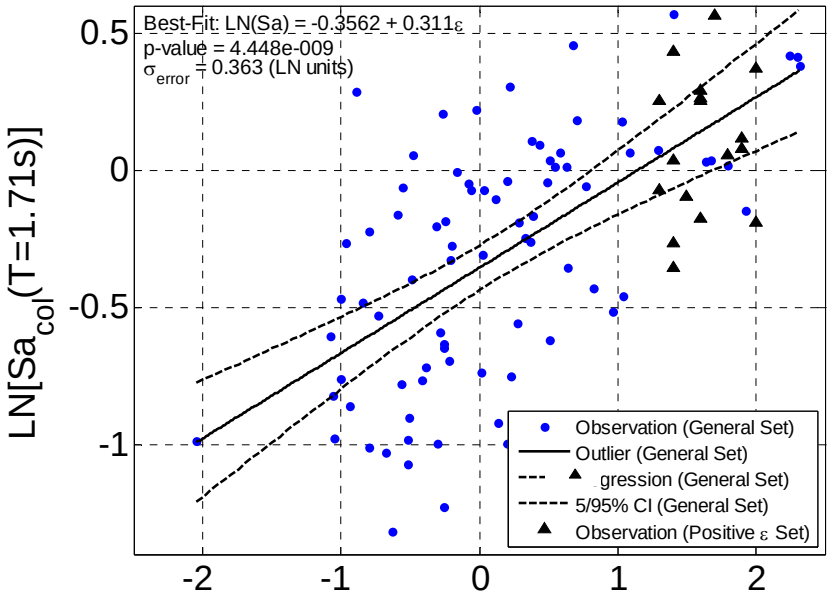

Figure 10. Relationship between spectral acceleration and ε, from Figure 8, but also including the collapse results predicted when directly using the Positive ε Set of ground motions.

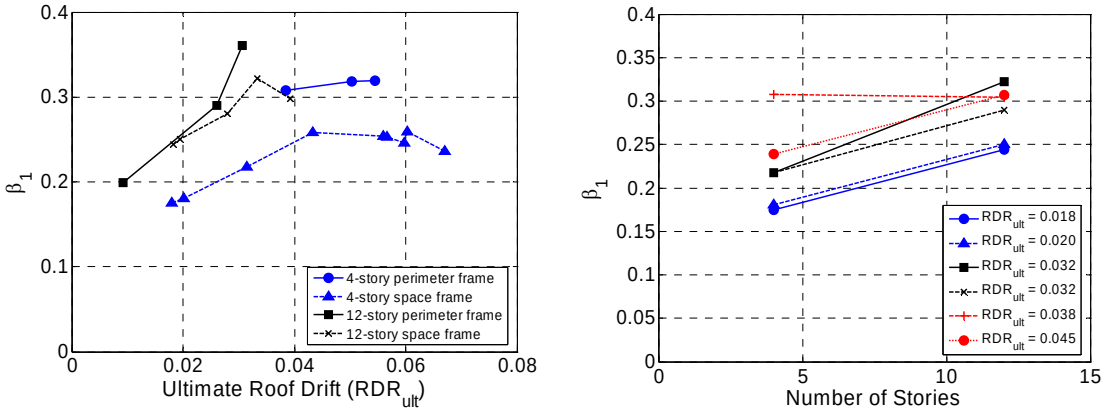

Figure 11. Relationship between (a) β_1 and building deformation capacity (RDR_{ult}), and (b) β_1 and number of stories.

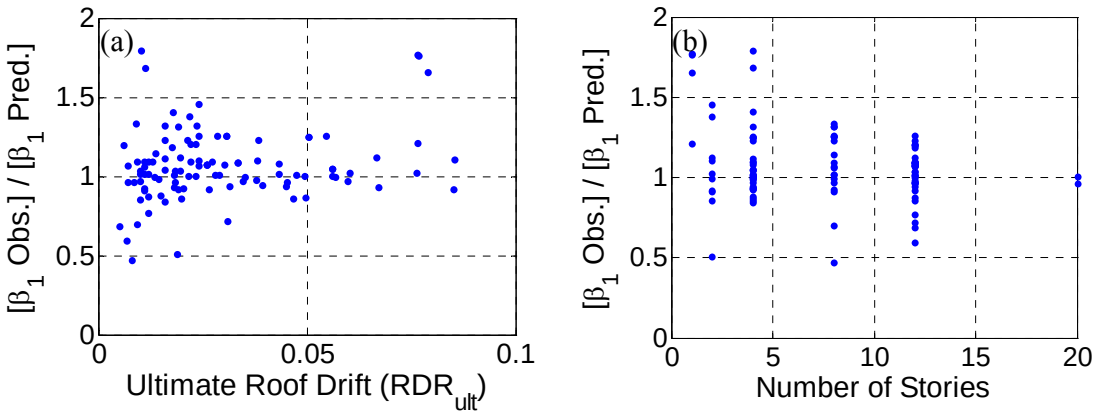

Figure 12. Ratio of observed/predicted β_1, plotted against (a) building deformation capacity (RDR_{ult}), and (b) number of stories.

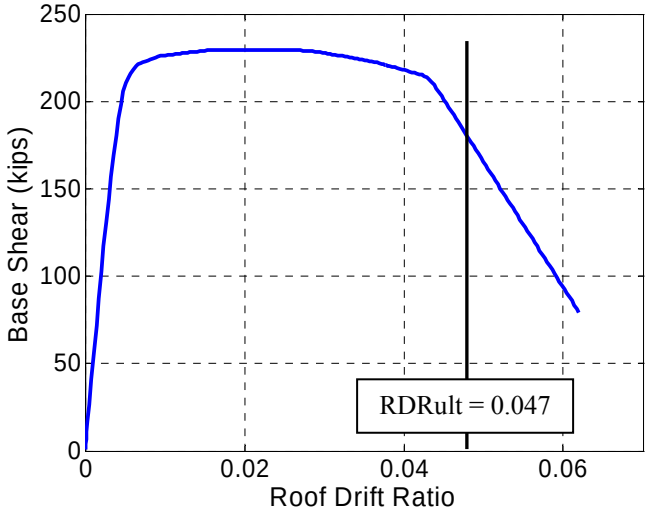

Figure 13. Static pushover curve for an example 4-story RC SMF building (ID 1008).

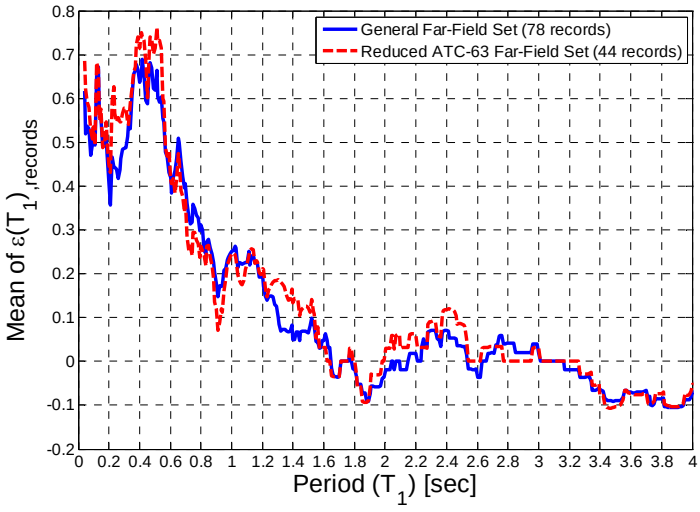

Figure 14. Mean ε values for the full and reduced versions of General Set of ground motions [$\overline{\varepsilon}(T_1)_{,\text{records}}$].